Acta Cryst. (1985). A41, 41-48

Multilayer Thin Films as Polarizing Monochromators for Neutrons

BY C. F. MAJKRZAK AND L. PASSELL

Physics Department, Brookhaven National Laboratory, Upton, NY 11973, *USA*

(*Received* 20 *February* 1984; *accepted* 20 *July* 1984)

Abstract

Recent progress in the development of polarizing multilayer thin-film monochromators for neutrons is reported. In particular, multilayers consisting of thin films of Fe and Ge with bilayer thicknesses of the order of 50 Å have been made with high peak reflectives and polarizing efficiencies. The results of measurements of multibilayer reflectivity and polarizing efficiency are compared with other neutron polarizers. A picture of the microscopic structure of the individual Fe and Ge films has also been obtained. Finally, practical applications of polarizing multibilayers are discussed.

1. Introduction

Possessing a magnetic moment, the neutron is a unique probe of the microscopic structure and dynamics of condensed-matter systems in which the constituent atoms or nuclei have spin-dependent cross sections. Full utilization of the discrimination afforded by the neutron moment can, nonetheless, require both a polarized incident beam and polarization analysis of the scattered neutrons, as demonstrated in the fundamental paper by Moon, Riste & Koehler (1969). Consequently, this powerful technique has in the past been restricted primarily to elastic scattering experiments because of the relatively low reflecting efficiencies of most existing polarizing monochromators. At present, the best commercially available polarizing monochromators are Heusler alloy crystals with typical reflectivities (for a single neutron spin state), which are approximately one-third to one-half that of the best nonpolarizing monochromators such as pyrolytic graphite (PG). Thus, for a conventional triple-axis spectrometer, the relative intensity loss due to the lower Heusler monochromator and analyzer reflectivities, combined with the automatic loss of one spin state upon initial polarization, can be a factor of 8 to 18! Although significantly higher Heusler crystal reflectivities have recently been reported (Freund, Pynn, Stirling & Zeyen, 1983), such crystals are not now generally available.

Recently it has been demonstrated that a new type of neutron polarizer can be fabricated of multibilayer thin films where one of the two film materials is ferromagnetic. In fact, two general types of multibilayer polarizing devices currently exist. One device, here referred to simply as a 'multilayer', consists of a number of bilayers of a single thickness or a distribution of thicknesses, which result in a diffraction peak at a position in reciprocal space separated from the region of total mirror reflection. Multilayer polarizers consisting of a number of bilayers of a single thickness or 'D spacing' were first reported by Lynn, Kjems, Passel, Saxena & Schoenborn (1976) and Hamelin (1976). The other type of multiple-thin-film polarizing device has become known as a 'supermirror' because it is composed of a particular sequence of bilayer thicknesses, which in effect extend the region of total mirror reflection beyond the ordinary critical angle. This concept was introduced by Turchin (1967) and Mezei (1976).

In the present paper we report on progress in the development of polarizing FeGe multilayers with average bilayer thicknesses of the order of 50 to 100 Å. These multilayers are found to have high reflectivities and polarizing efficiencies. Furthermore, by depositing a distribution of bilayer thicknesses it is shown that the angular acceptance for a given neutron wavelength in a divergent incident beam can be significantly increased over that obtained for a single-spacing multilayer. A picture of the microscopic structure of the individual Fe and Ge films that constitute the multilayer is presented and practical applications of multilayers as polarizers are discussed.

A more general review of the development of multilayers and supermirrors for neutron scattering instrumentation, which includes nonpolarizing applications, is given by Majkrzak (1984).

2. Multilayer fabrication

The FeGe multilayers reported on in this paper were made by sputter deposition. There are a number of reasons why sputtering is preferable to evaporation as a deposition technique. For example, deposition can be maintained at a relatively constant rate over periods of many hours or even days. Also, most materials, including those with high melting points and insulators, are readily sputtered. A general discussion of sputtering techniques is given by Vossen & Kern (1978). Details of the sputtering apparatus

0108-7673/85/010041-08$01.50

used to fabricate the FeGe multilayers reported on here are given by Saxena & Majkrzak (1984).

3. Reflectivity

In the Bragg reflection process for an ideally imperfect mosaic crystal bathed in a uniformly polychromatic beam, the wavelength resolution $\Delta\lambda/\lambda$ is given by $\cot\theta\Delta\theta$, where the spread in angle $\Delta\theta$ is due to both the crystal mosaic and the divergence of the incident beam. For a multilayer, on the other hand, $\Delta\lambda/\lambda = \cot\theta\,\Delta\theta + \Delta D/D$, where now $\Delta\theta$ is principally due to beam divergence alone and D is the average bilayer thickness. If for the moment any intrinsic width is neglected, ΔD is a measure of the width of some distribution of sets of bilayers of different thicknesses, which in effect scatter radiation of a given wavelength coherently over an extended angular range. (Random bilayer thickness variations of the type that give rise to a static Debye-Waller factor do not produce a broadening of a reflection in angle.) Even if $\Delta D/D$ is small, $\Delta\lambda/\lambda$ can be relatively large for practical beam divergences since θ is small and $\cot\theta$ correspondingly large. As discussed in § 6, there are a number of ways that the wavelength resolution can be sharpened without restricting the angular divergence of the beam to a prohibitive degree. Although a multilayer with a single D spacing reflects a relatively broad band of wavelengths, it reflects a given wavelength over a relatively limited angular range. In most cases, it is desirable to extract a given wavelength or range of wavelengths from a divergent incident beam at every possible angle. The angular acceptance of a multilayer for a given λ can, in fact, be made to match a particular beam divergence by creating a distribution of bilayer thicknesses. From this point of view the reflecting power or efficiency of a multilayer can be characterized by two measurable parameters, namely the peak reflectivity and angular acceptance for a single neutron wavelength.

The kinematical and dynamical theories of diffraction as applied to thin-film multibilayers have been discussed by Saxena & Schoenborn (1977) and Sears (1983). In the kinematical limit the reflectivity is proportional to the fourth power of the bilayer thickness D, the square of the number of bilayers N, and the reciprocal of the fourth power of the order of the reflection m. The width of the reflection in Q, where $Q = |\mathbf{Q}| = |\mathbf{k}_f - \mathbf{k}_i|$ and $\mathbf{k}_i$ and $\mathbf{k}_f$ are the incident and scattered neutron wavevectors, respectively, is also approximately proportional to $1/N$. If one material B of the bilayer is of thickness $D/2$ and is ferromagnetic and magnetized to saturation by an applied field $\mathbf{H}$ perpendicular to the momentum transfer $\mathbf{Q}$, then the reflectivity R is proportional to

$$[N_A b_A - N_B(b_B \pm p_B)]^2 \qquad (1)$$

where N_A and N_B are the atomic densities of materials A and B and b and p denote nuclear and magnetic scattering lengths, respectively. The plus (minus) sign preceding the magnetic scattering length corresponds to one (or the other) spin eigenstate of the incident neutron. If the scattering lengths and densities of materials A and B are properly chosen, then neutrons in one spin state see a uniform refractive index and $R = 0$ while those in the other spin state see a periodic modulation of the refractive index and a non-zero reflectivity when the Bragg condition is satisfied. This is the polarizing action of a multilayer. Although the kinematic theory is useful in understanding some of the essential properties of multilayers, extinction cannot always be neglected and dynamical theory is required.

3.1. *Reflectivity measurements*

A mosaic crystal can be described in terms of an angular disbribution of perfect microcrystallites, which reflect a given wavelength over a finite range of incident angles. The angular acceptance of a multilayer (with parallel layers) depends, for a particular wavelength, not on an angular mosaic but on a distribution of bilayer thicknesses or D spacings. Ideally, to measure directly the peak reflectivity and angular acceptance requires a perfectly parallel and monochromatic incident beam of radiation. In the case of a mosaic crystal, a rocking curve is then taken. (It is assumed that the natural or Darwin width of an individual microcrystallite is much narrower than the width of the angular distribution of the microcrystallites and that the aperture of the detector intercepts all of the radiation diffracted by a single microcrystallite.) For multilayers, on the other hand, a $\theta:2\theta$ scan is appropriate.

In practice, the peak reflectivity and angular acceptance of a multilayer for a given wavelength is measured on a spectrometer where the beam incident on the sample has a finite energy width and angular divergence. Reflectivity measurements were performed on a number of multilayers with various spectrometer configurations and degrees of resolution. For magnetized FeGe multilayers with several hundred bilayers and a D of the order of 50 Å, peak reflectivities approaching 0·90 with Q widths of 0·10 $Å^{-1}$ full-width at half-maximum (FWHM) have been obtained. This Q width is greater than that that would be expected for a single bilayer thickness and corresponds to a distribution of thicknesses arising from changes in deposition rate during fabrication. Fig. 1 compares the reflectivity of an FeGe multilayer consisting of almost 1500 bilayers of average thickness equal to 55 Å with that of pyrolytic graphite and Heusler alloy mosaic crystals. These measurements were performed on a standard triple-axis spectrometer in the elastic scattering mode without an analyzer and using a Heusler crystal as mono-

chromator (in conjunction with a pyrolytic graphite filter) to obtain a highly monoenergetic polarized beam incident on the sample. Preceding and following the sample were two pairs of single vertical slits giving collimations of 3· and 30′, respectively. The wavevector resolution Δk of the beam incident on the sample was $\simeq 0{\cdot}06$ Å^{-1} FWHM for $k = 2{\cdot}609$ Å^{-1} and the corresponding Q resolution, ΔQ, approximately $0{\cdot}005$ Å^{-1} FWHM for the multilayer and $0{\cdot}05$ Å^{-1} for the mosaic crystals. The incident beam width defined by the widths of the 3′ pair of slits was much narrower than the apertures of the 30′ pair of slits. The *minimum* value of the peak reflectivity is obtained by dividing the maximum diffracted intensity by that of the incident beam. In the case of the multilayer this was found to be 0·71. After deconvoluting the contribution of the instrumental resolution from the observed Q width of $0{\cdot}012$ Å^{-1} FWHM, an inherent width of approximately $0{\cdot}011$ Å^{-1} was obtained for the multilayer, which corresponds to an angular acceptance of about 7′ at $k = 2{\cdot}609$ Å^{-1}. The corresponding value of the peak reflectivity on deconvolution is 0·77. A good pyrolytic graphite crystal can have a peak reflectivity of about 0·75 and a width of 30′ at $k = 2{\cdot}609$ Å^{-1}. Thus the multilayer of Fig. 1 has approximately one quarter the integrated reflecting power of PG for a single wavelength. However, compared with the Heusler crystal of Fig. 1, the multilayer is clearly superior. The measurements described above were repeated at a wavevector of $1{\cdot}55$ Å^{-1} with consistent results. A calculation of the peak reflectivity and angular acceptance using the optical theory, described in the following section, predicts a peak reflectivity of about 0·75 and a width of $0{\cdot}0017$ Å^{-1} FWHM or 1·2′ at $2{\cdot}5$ Å^{-1} for a multilayer consisting of 100 bilayers with $\bar{D} = 50$ Å (25 Å Ge layer and 25 Å Fe layer) and random fluctuations of magnitude $\Delta D/D = 0{\cdot}05$ FWHM. In addition to the random fluctuations in bilayer thickness which occur during deposition of the films, relatively slow changes in deposition rate also take place. Whereas the former rate fluctuations result primarily in a decrease in peak reflectivity, the latter cause the broadening of the diffraction peak that is actually observed.

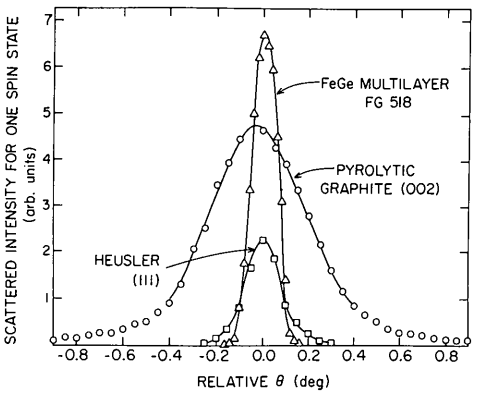

Fig. 1. Measured reflectivities and angular acceptances for an FeGe multilayer (FG518), pyrolytic graphite crystal (002 reflection) and Heusler crystal (111 reflection, reflection geometry) at $k = 2{\cdot}609$ Å^{-1} for one neutron spin state. In the case of the mosaic crystals, θ is the angle the crystal makes with the incident beam in a rocking curve whereas in the case of the multilayer θ is the angle made relative to the incident beam in a θ:2θ scan.

Table 1 summarizes the relevant properties of a representative sampling of FeGe multilayers. The values of the peak reflectivity given therein are uncorrected and, consequently, minimum values. The widths or angular acceptances are, on the other hand, the deconvoluted values, which are less than the widths actually observed. The uncertainties in the values of the widths appearing in Table 1 are of the order of 20%. The uncertainties in the measured reflectivities are of the order of 5%. The values given for the average Fe and Ge individual film thicknesses were determined gravimetrically by weighing, before and after deposition, a glass slide exposed to only one or the other sputter source and do not reflect the amount of interdiffusion which might have occurred. These measurements are uncertain by a few percent. The values for the average bilayer thickness determined directly from the position of the observed diffraction peak have not been corrected for the slight shift caused by refraction. Note that some of the multilayers in Table 1 have significantly broader angular acceptances. This was achieved by deliberately changing the bilayer thickness during deposition. However, because the total number of bilayers is presently limited by adhesion problems to about 1500, the peak reflectivity is consequently reduced.

In addition to the reflectivity measurements described above, separate rocking-curve data were obtained with collimations (again defined by pairs of single slits) of 1 and 2′ before and after the multilayers respectively. For the majority of multilayers deposited on float glass substrates, the rocking-curve width was found to be no greater than the divergence allowed by these collimations. The observations are consistent with a picture in which the bilayers composing the multilayer are in effect parallel to one another and to a flat substrate.

Fig. 2 compares the FeGe multilayer (FG518) shown in Fig. 1 with the supermirror and mirror described by Schärpf (1982). The supermirror effectively extends the critical angle for total mirror reflection (which is proportional to wavelength) by about two to two and one-half times that of an Ni mirror. This is the present practical limit according to Schärpf (1982). The supermirror reflects all wavelengths over a continuous range of angles up to the critical angle for each wavelength. However, as discussed at the beginning of this section, a multilayer also reflects a relatively broad band of wavelengths in a moderately divergent beam. The essential difference between supermirrors and miltilayers is that the latter give rise

Table 1. *Properties of a representative sampling of* FeGe *multilayers made to date*

Peak reflectivity values given are those obtained prior to deconvolution of spectrometer resolution and therefore represent minimum values.

Multilayer No. FG	Average film thickness (Å) Gravimetric determination Ge	Fe	Bilayer	Via neutron diffraction bilayer	Number of bilayers	Peak reflectivity for (+) spin state	Γ FWHM ($Å^{-1}$)	Flipping ratio
225 A	44	23	67	67	500	0·49	0·015	17
234 GA	50	39	89	87	900	0·82	0·011	18
412	29	20	49	52	1482	0·54	0·006	14
413	28	27	55	52	1246	0·62	0·011	18
502	—	—	—	50	669	0·24	0·034	20
503	—	—	—	68	1493	0·72	0·012	28
506	—	—	—	67	1082	0·60	0·012	14
512	36	29	65	69	1067	0·70	0·010	30
515	44	37	81	75	1037	0·71	0·012	22
516	39	55	94	92	1531	0·65	0·010	9
518	29	25	54	55	1478	0·71	0·011	6
520	—	—	—	108	10	0·23	0·008	37; 237*

* Result of a separate, more accurate measurement of the polarizing efficiency described in the text.

to distinct Bragg reflections at angles separated from the region of total mirror reflection. It is sometimes advantageous to utilize the higher scattering angles obtainable with multilayers, especially when working with shorter-wavelength neutrons. An additional advantage is that multilayers suppress higher-order wavelengths.

Note, however, that the FeAg supermirror of Fig. 2 has an angular acceptance of approximately 0·045 $Å^{-1}$ for the up spin state, whereas that of the FeGe multilayer is only 0·010 $Å^{-1}$. In many applications the most important requirement is to match the angular acceptance of the polarizing element for a given wavelength or range of wavelengths to the angular divergences of a beam without significant loss in peak reflectivity. As mentioned above, one means of accomplishing this in the case of a multilayer is to create a distribution of bilayer thicknesses centred about some particular average bilayer thickness.

3.2. *Bilayer thickness distributions*

The diffraction pattern that results for a given sequence of bilayer spacings can be calculated in a straightforward manner taking into account extinction, absorption and refraction. The method of calculation is analogous to that encountered in the solution of thin-film optical interference problems and has been used to study supermirrors; see, for example, Croce & Pardo (1970), Schelten & Mika (1979) and Yamada, Ebisawa, Achiwa, Akiyoshi & Okamoto (1978). The neutron is treated as a plane wave incident upon a layered but continuous medium with a corresponding Kronig–Penney-type periodic potential: boundary conditions are imposed at each interface and the reflection and transmission coefficients subsequently evaluated. The problem is conveniently formulated in matrix algebra for numerical computation. In our calculations we have incorporated random as well as systematic fluctuations in bilayer thicknesses. Absorption is also taken into account although the actual neutron path lengths are short enough and the cross sections for Fe and Ge sufficiently small that absorption and scattering (other than that which gives rise to the low-angle Bragg peaks) is usually negligible. It should be noted, however, that one possible limitation of this calculation is that it assumes an incident neutron plane wave and a multilayer structure of perfect uniformity and infinite extent parallel to the substrate.

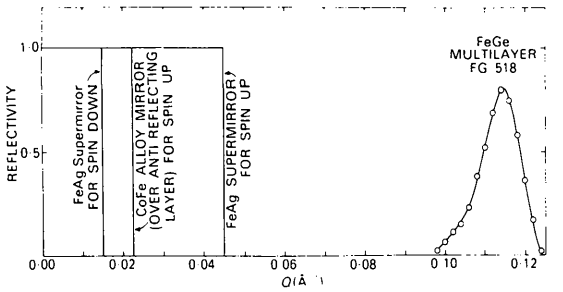

Fig. 2. Comparison of the FeGe multibilayer of Fig. 1 (FG518) with the supermirror and mirror of Fig. 3, Schärpf (1982). With the use of an antireflecting and absorbing layer between substrate and supermirror, the reflectivity of the FeAg supermirror for the spin-down eigenstate can be suppressed (private communication with O. Schärpf).

Several sequences of bilayer thicknesses have been proposed for supermirrors by Mezei (1976), Schelten & Mika (1979) and Yamada *et al.* (1978). In general a relatively large number of bilayers is required.

Using two simple relations from kinematic theory regarding the dependence of peak width and reflectivity on bilayer thickness and number of bilayers to create an algorithm for the bilayer thickness distribution, a calculation of the reflectivity as a function of Q for a distribution of 40 different bilayer thicknesses was performed using the optical method described above. The mean bilayer thickness was approximately 46 Å. A Gaussian distribution of random fluctuations

with an uncertainty of about 3% (FWHM) was also assumed. The calculation predicts that an average peak reflectivity for one spin state of about 0·90 extending over a range of approximately 0·025 $Å^{-1}$ can be obtained for a total of 2336 bilayers. For random errors of about 7%, significant dips in the peak reflectivity, down to almost 0·50 were calculated. This shows that control over random fluctuations is important. In practice the fluctuations can be monitored by an oscillating quartz crystal, whose frequency of vibration changes as material is deposited on it, making feedback control over deposition rates possible. It is worth noting that the random fluctuations can be of two different kinds. If the *total* thickness of the multilayer is monitored continuously and controlled to an uncertainty ΔD of a single bilayer thickness, then the random fluctuations in the multibilayer system will give rise to a static Debye–Waller factor. The intensity of the first Bragg reflection and higher-order harmonics will be diminished in intensity but the peak widths will be unaffected. If, instead, each individual bilayer is deposited with the same uncertainty ΔD but without monitoring the net thickness of the preceding bilayers, then there will be no long-range order since the distance from each successive bilayer to the substrate is more poorly defined (see for example Axe, 1976, p. 512). In this case the intensities and the widths of the higher-order reflections are affected. For the calculations discussed above, errors or the latter kind were assumed.

In summary, multiple-D-spacing multilayers with increased angular acceptance and of high reflectivity can and have been made. However, at present the angular acceptance cannot be increased significantly beyond 0·010 $Å^{-1}$ without a corresponding loss in peak reflectivity because of the present limitation on the total number of bilayers that can be deposited ($\simeq$1500) on a single substrate. In order to increase the maximum number of bilayers that can be deposited, experimentation with different materials (*e.g.*, Fe and W), substrates (*e.g.* Si or Al_2O_3) and sputtering conditions is now being done.

Another possible means of manufacturing a multiple-D-spacing multilayer is to deposit the required N' bilayers of spacing D' on one substrate, N'' bilayers of spacing D'' on another substrate, and so on, and then to superimpose the substrates on one another in a parallel orientation. If the substrate material is perfect-crystal Si or Al_2O_3, then the substrates will be nearly transparent even for the relatively long path lengths at small angles through minimum substrate thicknesses. Alternatively, several substrates on each of which are deposited N bilayers of the same D spacing can be superimposed on one another but at different angles, which are a fraction of the angular width of each individual element. This latter arrangement would be similar to a mosaic crystal. In either configuration, however, the intensities scattered from the separate groups of bilayers would add incoherently. Extinction would then be secondary rather than primary.

Table 2. *Beam width and angular acceptance as a function of neutron wavelength or energy for a multilayer* 50 cm *long with an average* D *of* 50 Å *and a* Γ *of* 0·010 $Å^{-1}$ *FWHM*

λ (Å)	E (meV)	Maximum beam width (cm)	Angular Acceptance Γ (FWHM) (′)
1·65	30	0·8	4·5
2·34	15	1·2	6·4
4·04	5	2·0	11·1
6·40	2	3·2	17·5
9·04	1	4·5	24·8

3.3. *Other multilayer properties*

Once the peak reflectivity, polarizing efficiency and angular acceptance of a multilayer have been optimized, there remain secondary geometrical considerations regarding, for example, beam dimensions or the relative uniformity of the multilayer film at different points on the surface of the substrate. For the FeGe multilayers deposited on 2×18×0·25 in thick (5·08×45·72×0·635 cm) float glass substrates, a relative uniformity in thickness to within a few percent has been obtained. With more sophisticated feedback control of the deposition rates, even greater uniformity should be possible if required. It might be useful to note here that, as would be expected, the peak reflectivity is found to be practically independent of vertical beam divergences of the order of a degree. Table 2 is a compilation of maximum horizontal beam dimensions and angular acceptances as a function of neutron wavelength and energy for a bilayer thickness of 50 Å, a substrate length of 50 cm, and a ΔQ of 0·010 $Å^{-1}$ FWHM. Of course, it is possible to reduce significantly the length of a multilayer required for a given beam width by assembling a straight or bent Soller array of multilayers as is done, for example, by Schärpf (1982) with supermirrors.

4. Polarizing efficiency

If it is assumed that the Fe and Ge thin films comprising a multilayer have the same respective densities as in the bulk and form well-defined interfaces with no interdiffusion, then the flipping ratio R of the intensity of neutrons diffracted with spin up to that of neutrons with spin down is given in the kinematic limit to be 217. This corresponds to a polarizing efficiency P of 0·9954. Fe is a particularly good material to use as the ferromagnetic layer since it has a relatively large moment and high atomic density, is magnetically soft and can be deposited in thin films of high quality. Ge has the appropriate density and

nuclear scattering length to match those of Fe closely for the spin-down state. However, a number of other elements, in principle, could be used. Potentially, Se, W and Zr used instead of Ge would give better flipping ratios ($R \simeq 43\,000$, 25 000 and 20 000 respectively). Furthermore, alloy compositions could be used to 'fine tune' the matching of refractive indices.

In the kinematic limit the polarizing efficiency is independent of the number of bilayers, the D spacing, and the relative thicknesses of the films of the two materials. Diffusion and extinction can, however, affect the polarizing efficiency.

Measurements of the polarizing efficiencies or flipping ratios of the FeGe multilayers included in Table 1 were performed using the same spectrometer configuration as that described above for the reflectivity measurements. However, the polarizing efficiency of the Heusler crystal monochromator in this particular arrangement was limited by a magnetic field of about 0·13 T, which was insufficient for saturation. Thus, the measured flipping ratios quoted in Table 1 are actually lower than the true values, the difference being larger for the multilayers with the higher measured flipping ratios. It is found, on the other hand, that the Fe layers of a multilayer can be nearly saturated in magnetic fields of the order of 0·01 to 0·03 T.

The relatively low polarizing efficiencies of some of the multilayers included in Table 1 can be attributed to the effect of primary extinction. This effect can of course be minimized by reducing the number of bilayers of a given thickness or by better matching of refractive indices as discussed above.

A separate polarizing efficiency measurement using a different spectrometer configuration was made on FG520 with a smaller Heusler crystal (as analyzer) placed in a larger field of 0·25 T, which was sufficient for saturation. Fig. 3 is a plot of intensity *vs* Q for the FeGe multilayer (FG520) with $N = 10$ bilayers and $D = 108$ Å as measured at a neutron wavevector of 2·609 Å^{-1}. The intensities I_+ and I_-, for spin-up and spin-down neutrons respectively, are measured sequentially at the same value of Q without moving the spectrometer. At $Q = 0{\cdot}057$ Å^{-1}, the flipping ratio $R = I_+/I_-$ is found to be 237. The kinematical prediction is 217. However, according to the optical theory discussed in § 3.2, a shift in the relative positions of the peaks corresponding to spin-up and spin-down neutrons is predicted owing to refractive-index differences for the two spin states. This causes an oscillatory behavior of the flipping ratio as the first-order peak and subsidiary maxima for one spin state are out of phase with those of the other. In practice, the instrumental resolution and bilayer thickness fluctuations usually obscure the finer details of this effect although shifts in the positions of the principal maxima are still observed (for N bilayers there will be $N-1$ minima between Bragg reflections of successive orders: see, for example, Fig. 9 of Saxena & Schoenborn, 1977). Because of these shifts the flipping ratio at some values of Q can be even greater than that predicted by the kinematical structure factor.

Closer inspection of Fig. 3 also reveals that the reflected intensity for spin-up neutrons becomes *less* than that for spin-down at the second- and fourth-order positions (the fact that there is some intensity at the even-order Bragg positions indicates that the Fe and Ge layers are not of exactly equal thickness). It can be shown that this reversal cannot occur for a multilayer where the magnetic scattering-length density is uniform throughout the Fe layer (this is true in both the kinematic and optical theories). However, if a region of interdiffusion between Fe and Ge occurs or the ordered Fe moments at the interface have a different magnitude from those at the interior of the layer, then such behavior can be explained. This will be discussed further in § 5.

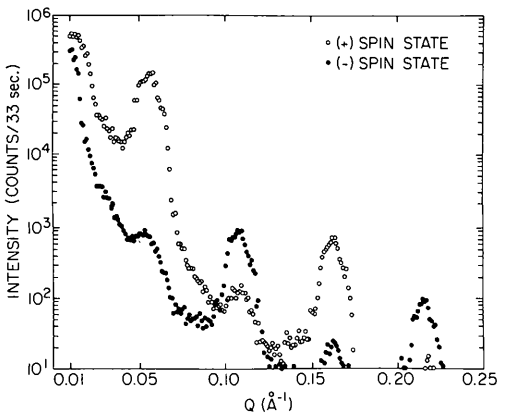

Fig. 3. Intensity data as a function of Q for an FeGe multilayer (FG520) with ten bilayers and an average bilayer thickness of 108 Å. Positive spin-state intensity is plotted with open circles and that corresponding to the negative spin state with solid circles.

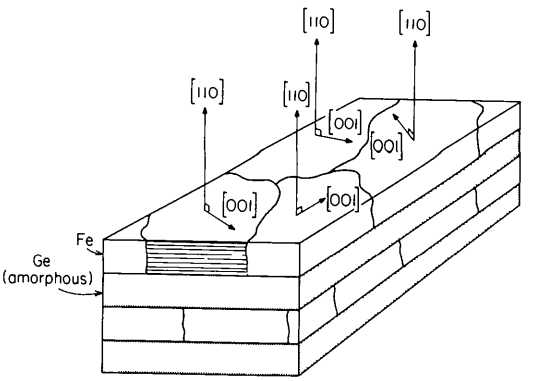

Fig. 4. Approximate picture of the microscopic chemical structure of the Fe and Ge films composing a multilayer based on X-ray diffraction data. Further investigation reveals significant diffusion across the interface between Fe and Ge films.

Finally, we mention that another advantage of multilayer polarizers is that the troublesome simultaneous reflection effects that occur in Heusler crystals and that often result in poor instrumental flipping ratios as discussed by Majkrzak & Shirane (1982) are avoided.

5. Microscopic structure of the films

In order to determine the microscopic structure of the Fe and Ge thin films in each bilayer, two X-ray diffraction patterns were obtained, one with the scattering vector in the plane of the substrate (transmission geometry), the other with the scattering vector perpendicular to the plane of the substrate (reflection geometry). The data clearly show that each Fe layer or film is made up of microcrystallites oriented with a [110] direction normal to the plane of the substrate but randomly rotated about this direction in a plane parallel to that of the substrate. The dimension of the Fe microcrystallites parallel to the plane of the substrate is estimated to be of the order of one to three hundred Å from a measurement of the width of the 110 diffraction peak in transmission geometry. However, because the inherent width of the diffraction peak (obtained by deconvoluting the instrumental width from the measured width) is inversely proportional to the coherence length, it is difficult to distinguish the contribution to this width that is due to the finite size of the microcrystallite from that that is caused by strain. Separate rocking-curve scans indicate that the angular distribution of [110] directions has a FWHM of approximately 9° centered about the normal to the plane of the substrate.

The Ge film, on the other hand, is found to be amorphous owing to the absence of any powder diffraction lines in either reflection or transmission geometry.

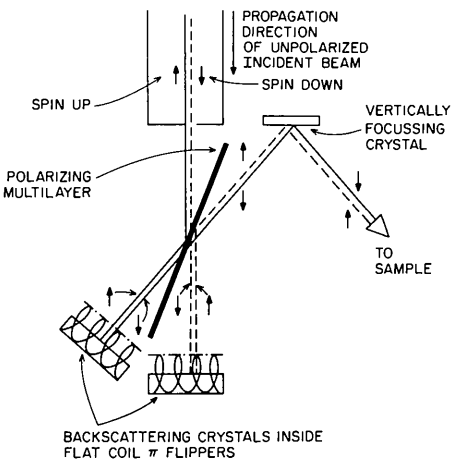

Fig. 5. Polarizing multilayer used for extraction of a back-scattered beam as described in the text.

The general picture of the microscopic structure of the multilayer that then emerges is shown schematically in Fig. 4. A more detailed plot of an Fe 110 peak obtained in reflection geometry using X-rays reveals a satellite structure centered about the principal maximum, which can be shown to be a consequence of the relatively small finite number of Fe (110) planes comprising a single Fe layer. The satellite spacing is in fact a direct measure of the number of Fe (110) planes per layer.

The Fe 110 diffraction peak in reflection geometry can also be seen with polarized neutrons. Although a satellite structure is again observed, there is a significant difference between the profiles corresponding to $|F_N + F_M|^2$ measured by spin-up neutrons and $|F_N - F_M|^2$ measured by spin-down neutrons, where F_N and F_M are the nuclear and magnetic structure factors, respectively. This data, together with the flipping ratios of the first- and higher-order superlattice reflections at low angles, can be fit to a model where in addition to a region of Fe (110) planes there exists a number of FeGe alloy planes of varying degrees of relative concentration. In the alloy planes, the Fe moments are reduced in magnitude. On annealing it is found that interdiffusion increases to the extent that the entire multilayer becomes FeGe alloy but with a single preferred orientation of one crystallographic direction normal to the plane of the substrate remaining. The coherence length in that direction normal to the substrate plane is also greatly increased.

A more complete report on the investigation of the microscopic structure of the Fe and Ge films will be forthcoming (Majkrzak, Axe & Böni, 1984).

6. Practical applications of polarizing multilayers

A simple yet effective way to improve the relatively poor energy resolution of a multilayer (if necessary to do so) is to use it in conjunction with a crystal monochromator such as pyrolytic graphite. The pyrolytic graphite does the monochromating and the multilayer the polarizing. This combination has in fact been successfully employed here at Brookhaven.

However, once a neutron beam has been polarized, other, more innovative and advantageous means can be used to sharpen the energy resolution. One such scheme utilizes a wavelength-dependent flipping device of the kind first proposed by Drabkin (1962) and is discussed by Aganalyan, Drabkin & Lebedev (1977) and by Majkrzak & Shirane (1982). This device has the remarkable property that the energy width is essentially decoupled from the angular divergence of the beam. The energy resolution and divergence of the beam can then be selected independently to suit a particular experiment.

Another application where polarizing multilayers can be used to advantage involves a back-scattering spectrometer. Consider the back-scattering configur-

ation shown in Fig. 5. An unpolarized beam of nominal wavelength λ is incident upon a polarizing multilayer set at the appropriate Bragg angle. The spin-up neutrons are reflected while the spin-down neutrons are transmitted (the multilayer can be deposited on either a single substrate or a Soller array of substrates of highly transparent single-crystal Si or sapphire). The transmitted beam is subsequently back-scattered at exactly 90° from a mosaic crystal placed within a flat-coil spin flipper. The flipper field is adjusted so that within the coil a neutron makes an adiabatic $\pi/2$ turn before and a $\pi/2$ turn after being reflected. (The coil thickness can be made large compared to the average penetration depth of a neutron into the crystal.) The back-scattered neutron now in the 'up' eigenstate is subsequently deflected by the multilayer towards the sample (or, as shown in Fig. 5, a vertically focusing PG crystal and then to the sample). The spin-up neutrons in the incident beam, on the other hand, will be first reflected by the multilayer and upon back-scattering from another crystal undergo a π spin turn and be transmitted through the multilayer in the same direction as the original incident spin-down neutrons. The advantage of this arrangement is that the exact back-scattering geometry is maintained without the problems normally encountered in using an ordinary deflection crystal in the incident beam, which would deflect incident neutrons equally as well as back-scattered neutrons. Also, if needed, a polarized beam can be obtained by simply shutting off one or the other π-flipper.

It is a pleasure to acknowledge the contributions, either through discussion or technical assistance, of the following people at Brookhaven: J. D. Axe, E. Caruso, D. Cox, J. Hurst, F. Langdon, B. Lenz, F. Merkert, A. Moodenbaugh, P. E. Pyne, A. Saxena, B. P. Schoenborn, G. Shirane and R. Stoenner. Research at Brookhaven was supported by the Division of Materials Sciences, US Department of Energy, under contract no. DE-AC02-76CH00016 and NSF grant no. PCM77-01133.

References

AGANALYAN, M. M., DRABKIN, B. M. & LEBEDEV, V. T. (1977). *Zh. Eksp. Teor. Fiz.* **73**, 382-386.
AXE, J. D. (1976). *Physics of Structurally Disordered Solids*, edited by S. S. MITRA, pp. 507-524. New York: Plenum.
CROCE, P. & PARDO, B. (1970). *Nouv. Rev. Opt. Aple.* **1**, 229.
DRABKIN, G. M. (1962). *Zh. Eksp. Teor. Fiz. Pis'ma Red.* **43**, 1107-1108.
FREUND, A., PYNN, R., STIRLING, W. G. & ZEYEN, C. M. E. (1983). *Physica (Utrecht)*, **120B**, 86-90.
HAMELIN, B. (1976). *Nucl. Instrum. Methods*, **135**, 299-306.
LYNN, J. W., KJEMS, J. K., PASSEL, L., SAXENA, A. M. & SCHOENBORN, B. P. (1976). *J. Appl. Cryst.* **9**, 454-459.
MAJKRZAK, C. F. (1984). In preparation.
MAJKRZAK, C. F., AXE, J. D. & BÖNI, P. (1984). In preparation.
MAJKRZAK, C. F. & SHIRANE, G. (1982). *J. Phys. (Paris) Colloq.* C7, 215-220.
MEZEI, F. (1976). *Commun. Phys.* **1**, 81-85.
MOON, R. M., RISTE, T. & KOEHLER, W. C. (1969). *Phys. Rev.* **181**, 920-931.
SAXENA, A. M. & MAJKRZAK, C. F. (1984). *Neutrons in Biology*, edited by B. P. SCHOENBORN, pp. 143-157. New York: Plenum.
SAXENA, A. M. & SCHOENBORN, B. P. (1977). *Acta Cryst.* A**33**, 805-813.
SCHARPF, O. (1982). *AIP Conf. Proc. No.* 89, edited by J. FABER, pp. 182-189. New York: American Institute of Physics.
SCHELTEN, J. & MIKA, K. (1979). *Nucl. Instrum. Methods*, **160**, 287-294.
SEARS, V. F. (1983). *Acta Cryst.* A**39**, 601-608.
TURCHIN, V. F. (1967). *At. Energ.* **22**, No. 2. Deposited paper.
VOSSEN, J. L. & KERN, W. (1978). *Thin Film Processes*. New York: Academic Press.
YAMADA, S., EBISAWA, T., ACHIWA, N., AKIYOSHI, T. & OKAMOTO, S. (1978). *Annu. Rep. Res. React. Inst. Kyoto Univ.* **11**, 8-27.

Acta Cryst. (1985). A**41**, 48-55

A New Approach to the Measurement of X-ray Structure Amplitudes Determined by the *Pendellösung* Method

BY MOSHE DEUTSCH* AND MICHAEL HART

Wheatstone Laboratory, King's College, Strand, London WC2R 2LS, England

(*Received* 3 *November* 1983; *accepted* 27 *July* 1984)

Abstract

The Laue-case rocking curve from two thin crystals is known to exhibit fine structure which can be used to determine the corresponding structure amplitude F_h. Thus F_{444} and F_{777} have been measured for crystalline silicon to a standard deviation of 0·2%. F_{444} is in excellent agreement with published experimental values. There are no previous high-precision measurements of F_{777} in the literature. The values measured

* Permanent address: Department of Physics, Bar-Ilan University, Ramat-Gan, Israel.

0108-7673/85/010048-08$01.50